Advances in Engineering Software 190 (2024) 103598

Contents lists available at ScienceDirect

Advances in Engineering Software

journal homepage: www.elsevier.com/locate/advengsoft

Research paper

Robust improvement of the finite-element-model updating of historical constructions via a new combinative computational algorithm

Javier Naranjo-Pérez [a], Rubén Rodríguez-Romero [b], Pablo Pachón [c,*], Víctor Compán [c], Andrés Sáez [b], Aleksandar Pavic [d], Javier Fernando Jiménez-Alonso [b]

[a] Department of Continuum Mechanics and Structures, E.T.S. Ingenieros de Caminos, Canales y Puertos. Universidad Politécnica de Madrid, Madrid, Spain
[b] Department of Continuum Mechanics and Structural Analysis, Universidad de Sevilla, Seville, Spain
[c] Department of Building Structures and Ground Engineering, Universidad de Sevilla, Seville, Spain
[d] Vibration Engineering Section, College of Engineering, Mathematics and Physical Sciences, University of Exeter, Exeter, UK

ARTICLE INFO

Keywords:
Finite element model updating
Maximum likelihood method
Bi-objective optimization
Decision-making problems
Historical building stone

ABSTRACT

Finite-element-models are usually employed to simulate the behaviour of historical constructions. However, despite the high complexity of these numerical models, there are always discrepancies between the actual behaviour of the structure and the numerical predictions obtained. In order to improve their performance, an updating process can be implemented. According to this process, the value of the most relevant physical parameters of the model is adjusted to better mimic the actual behaviour of the structure. For this purpose, the actual structural behaviour is usually characterized via its experimental modal properties (natural frequencies and associated vibration modes). For practical engineering applications, the maximum likelihood method is normally considered to cope with this problem, due to its easy implementation together with an understandable interpretation of the updating results. However, the complexity of these numerical models makes unfeasible the practical implementation of the process due to the simulation time required for its computation. In order to shed some light to this problem, a new combinative computational algorithm is proposed herein. Additionally, the performance of the proposal has been assessed successfully via two applications: (i) a validation example, the model updating of a laboratory footbridge, in which the practical implementation of the algorithm has been described in detail; and (ii) a case-study, the model updating of a complex historical construction, in which the main advantage of the proposal has been highlighted, a clear reduction of the simulation time required to solve the updating problem without compromising the accuracy of the solution obtained.

1. Introduction

Finite element (FE) method is usually employed to simulate numerically the structural behaviour of historical constructions [1]. However, despite the great complexity of these models [2], there are always differences between the predictions provided by these numerical tools and the actual behaviour of the structure [3]. These differences are normally originated by some of the following sources of errors and uncertainty [4]: (i) the approximate solution of differential equations that governs the dynamic behaviour of a structure (numerical uncertainty); (ii) the imprecise value of the model input parameters (parameter uncertainty); (iii) the incomplete definitions of underlying physics due to assumptions and idealizations (bias error); and (iv) the variability in measurements (experimental uncertainty).

In order to reduce the effect of these sources of uncertainty, the FE model updating method is normally considered [5]. According to this method, some physical parameters of the FE model are modified in order to better mimic the real behaviour of the structure. In the case of complex historical construction, the updated FE model is usually employed both to better assess the static or dynamic response of the structure and to establish a damage detection application based on a structural health monitoring strategy.

Different criteria can be considered for the classification of the FE model updating methods. Regarding the time available for its computation, two types of methods can be considered: (i) off-line methods; and (ii) on-line methods. Thus, under the off-line approach, the FE model of the structure is directly updated via the modification of the value of its most relevant physical parameters. A high computational time is normally required to solve the updating problem according to his approach. This method is usually used to improve the accuracy of FE model when they are employed to assess the structural behaviour of

* Corresponding author.
E-mail address: ppachon@us.es (P. Pachón).

https://doi.org/10.1016/j.advengsoft.2024.103598
Received 29 August 2023; Received in revised form 1 February 2024; Accepted 2 February 2024
Available online 6 February 2024

civil engineering structures and historical constructions [2]. In addition, under the on-line approach, the FE model is approximated via a subrogate model and subsequently this model is calibrated according to some updating method. The use of this subrogate model allows reducing the simulation time required to solve the updating problem. This method is commonly used to damage detection under structural health monitoring strategies [6]. In this manner, the main difference between this two type of updating methods is related to the considered numerical model. Therefore, the same process is commonly employed to solve the updating problem for this two methods. This study is focused on the off-line updating approach, but its results can be easily extrapolated to the on-line approach.

Additionally, FE model updating problems can be classified, regarding the parameter selection, in two main groups [7]: (i) direct methods (non-iterative) and (ii) indirect methods (iterative).

On the one hand, according to the direct methods, the updating parameters are directly the components of the matrices that constitute the system equations considered to numerically mimic the behaviour of the structures. The main advantage of these methods is its direct and easy implementation but they present a clear drawback, the non-physical meaning of the updated value of the parameters. On the other hand, according to the indirect methods, the updating parameters are some of the most relevant physical parameters of the structure (as for instance, Young's modulus of the materials, stiffness of the support ...) that are iteratively modified in order to adjust the predictions of the numerical model to the actual response of the structure. In contrast to the previous methods, the adjusting process is more complicated, being necessary the use of complex computational tools, but they presents as advantage an easy physical interpretation of the updated value of the considered parameters. This advantage allows that the updating process can be considered a system identification method and it has originated that iterative methods have been widely used for the FE model updating of building and civil engineering structures.

Among the indirect methods, a new classification can be established in terms of the quantification of the level of uncertainty. Two types of methods can be considered [7]: (i) deterministic and (ii) stochastics methods. Although, stochastics methods, as probabilistic [8] and fuzzy approaches, allow the determination of the level of uncertainty of the estimation of the updated values of the physical parameters [9], the high simulation time required to solve the updating problem, according to these approaches, have reduced, to date, their extensive practical implementation. For robust FE models of complex historical construction, deterministic methods are normally used.

Among the deterministic methods, the maximum likelihood method has been widely employed due to its easy implementation. According to this method, the updating problem can be formulated as either a sensitivity-based weighted single-objective optimization problem or the combination of a bi-objective optimization sub-problem and a decision-making sub-problem. Some recent results, [10] about the performance of both methods when they are implemented for the FE model updating of civil engineering structures; have concluded that the second alternative allows obtaining a better adjustment since this second method explores in detail all the domain space of the possible value of the considered physical parameters.

Therefore, the updating problem, according to this second method, is formulated considering a bi-objective function whose components are defined in term of the relative differences (residuals) between the experimental (actual) and numerical behaviour of the structure [11]. In order to characterize the actual behaviour of the structure, its experimental modal properties, identified considering either an experimental (EMA) [12] or operational modal analysis (OMA), are usually considered [13]. In this manner, these residuals are usually defined in terms of the relative differences between the experimental and numerical modal properties (natural frequencies and associated vibration modes) of the structure.

Additionally, as the relation between the updating parameters and this bi-objective function is clearly nonlinear and, as a consequence, multiple local minimums can be reached; global optimization algorithms must be used to solve this problem [14]. As result of this optimization process, a set of possible solutions is obtained, the so-called Pareto front [12]. Finally, a subsequent decision-making problem must be solved, the selection of the best balanced solution (the "knee" point) among the different elements of the Pareto front. For this purpose, different methods have been considered [15] without existing to date a unified criterion to cope with this problem.

In spite of all the advantages of the abovementioned method, when it is implemented to solve the FE model updating of complex historical construction structures, it presents a clear drawback, the high simulation time required to solve the problem. In order to improve the performance of this method, several numerical techniques can be adopted: (i) to increase the search speed of the optimization algorithm combining local and global computational optimization algorithms [16]; (ii) to reduce the complexity of the FE model approximating its behaviour via surrogate models [17]; (iii) to find the optimum selection of the physical parameters of the FE model; (iv) to use alternative mathematical tools to solve the updating problem more efficiently [7]; and (v) to use some clustering technique for the parallel computation of the updating problem [18].

This research study focuses in the first alternative, the proposal of a new combinative computational algorithm to reduce the simulation time required to perform the FE model updating of historical construction without compromising the accuracy of the solution obtained. For this purpose, this proposal takes advantage of the virtues of two previous algorithms [19,20], proposed by some of the authors of the manuscript, and it combines them to improve the efficiency of the updating process.

For this purpose, the proposed algorithm makes use of a local–global optimization algorithm, the UKF-MHS algorithm [19], both to increase the convergence speed of the searching algorithm and to reduce the uncertainty associated with the variability of the experimental measurements, together with a collaborative algorithm [20], which allows a robust estimation of the "knee" point via the linking of several statistical learning techniques. The combination between these two algorithms improves clearly the performance of the FE model updating of complex historical constructions. Thus, it is necessary to highlight that the main contribution of this paper is not only the combination of two previously reported algorithms to obtain an efficient computational tool that assists architects and structural engineers in the FE model updating of historical constructions but also its practical implementation in two examples. These application examples try to highlight the virtues of the proposal. First, this new algorithm has been implemented for the off-line FE model updating of a laboratory footbridge. In this manner, this first application example has been used as tutorial to explain in detail the different steps of this computational algorithm. Subsequently, the algorithm has been implemented for the off-line FE model updating of a complex historical constructive. In this second application example, the higher performance of the proposal in comparison with the abovementioned conventional bi-objective approach has been remarked.

In addition to this introductory section, the remaining paper is organized as follows. Section 2 describes both the basics of the FE model updating, according to the maximum likelihood method, and the formulation of the proposed new combinative algorithm. Section 3 focuses on the detailed description of the proposal via a validation example, the practical implementation of the algorithm for the FE model updating of a laboratory footbridge. Section 4 presents the performance assessment of this proposal when it is implemented for the FE model updating of a historical construction. For this purpose, the model updating of the church of the Royal Monastery of San Jerónimo (Granada, Spain) is developed in detail. Finally, Section 5 summarizes the main conclusions that can be drawn from the work.

2. Solving the maximum likelihood FE model updating problem via a new combinative computational algorithm

2.1. Basics of FE model updating according to the maximum likelihood method

The goal of FE model updating is to acquire a precise numerical FE model that corresponds to the experimental dynamic properties of the analysed civil or building engineering structure. This objective can be accomplished by approximating the most significant physical parameters of the model that reduce the differences between the numerical and experimental data (residuals). Consequently, the FE model updating issue can be interpreted as a parameter identification problem.

In this regard, the maximum likelihood method is the most commonly utilized estimator for civil or building engineering applications. Assuming that the residuals follow a normal distribution, the maximum likelihood method is analogous to the ordinary least squares method. Hence, the model updating can be converted into an optimization problem, whose primary goal is to reduce the total of the relative deviations between the experimental and numerical modal properties. Thus, the updating problem can be formulated alternatively as two different optimization problems [7]: (i) a sensitivity-based weighted single-objective optimization problem; or (ii) a combination of a bi-objective optimization sub-problem together with a decision-making sub-problem. Due to the higher efficiency of the second formulation [10] to cope with this problem, the multi-objective approach has been considered herein. The relevant physical parameters of the model are taken as the design variables for this purpose. Therefore, the formulation of the FE model updating issue considering the bi-objective approach can be represented as:

$$\min\left[f_1(\theta)\ f_2(\theta)\right] = \min\left[\frac{1}{2}\sum_{j=1}^{m_f} r_j^f(\theta)^2\ \frac{1}{2}\sum_{j=1}^{m_m} r_j^m(\theta)^2\right] \quad \theta_l \le \theta \le \theta_u \tag{1}$$

where r_j^f (θ) and rmj r_j^m (θ) refer to the discrepancies between the jth natural frequency and mode shapes of the structure and their theoretical counterparts; m_f represents the quantity of considered natural frequencies; m_m represents the quantity of considered mode shape; θ is a vector comprising the updating parameters of the FE model; and θ_l and θ_u denote the lower and upper limits of the exploration range for these physical parameters, respectively.

The residuals may be defined as:

$$r_j^f(\theta) = \frac{f_{num,j}(\theta) - f_{exp,j}}{f_{exp,j}} j = 1, 2, \ldots, m_f \tag{2}$$

$$r_j^m(\theta) = \sqrt{\left(\frac{\left(1 - \sqrt{MAC_j(\theta)}\right)^2}{MAC_j(\theta)}\right)} j = 1, 2, \ldots, m_m \tag{3}$$

considering the numerical natural frequency j as $f_{num,j}(\theta)$, the experimental natural frequency j as $f_{exp,j}(\theta)$, and the Modal Assurance Criterion value $MAC_j(\theta)$ [21] as a measure used to assess the similarity between the mode shapes of the numerical vibration mode j, $\varphi_{num,j}(\theta)$ and the experimental vibration mode j, $\varphi_{exp,j}(\theta)$. As the accuracy of the $MAC_j(\theta)$ ratio depends on the geometrical definition of the mode shapes, a sufficient refined gridline is needed to characterize the value of this magnitude [10]. For this purpose, a sensitivity analysis can be performed. In this study, the variation of the $MAC_j(\theta)$ ratio in term of the number of coordinates that defined the gridline (of the experimental identification test) is analysed in detail. A balanced value between the complexity of the gridline and the accuracy of the $MAC_j(\theta)$ ratio is taken into account.

The physical parameters of the updating process must be selected carefully since they condition the accuracy and reliability of the solution. Based on a FE model, a different updating problem can be formulated depending on the relation between the residuals and the considered updating parameters. For the parameter selection purpose, different criteria can be considered [7]. Among the different criteria, a sensitivity analysis is commonly employed. According to this study, the variation of the natural frequencies and mode shapes in term of the considered physical parameters is computed. As this variation is proportional to the modal strain energy this magnitude is considered to perform the sensitivity analysis. The physical parameters, which reflect a higher variation, are selected as updating parameters [10].

The resolution of this bi-objective optimization problem generates a set of parameter vectors, each representing a potential solution. These parameters can be visually represented by forming a curve known as the Pareto front. Each point along the Pareto front represents an optimal updated model where improving one objective would require sacrificing another. Consequently, selecting the best solution from the Pareto front requires a decision-making process. Several methods have been proposed in literature to tackle this challenge by balancing the different terms of the Pareto front. Generally, these methods identify the best solution on the Pareto front as the point where a slight improvement in one objective would significantly deteriorate the other objective. This particular point on the Pareto front is often referred to as the "knee" point, and each method suggests a slightly different criterion for its determination.

Following the above approach and under the maximum likelihood method, the FE model updating is usually addressed by implementing computational intelligence algorithms [22]. For this purpose, a FE analysis package is commonly linked to an optimization package. As illustration of this connectivity, Fig. 1 shows the flowchart of the updating process giving a special emphasis to the linking between the two abovementioned packages together with the flow of data. During the updating process, a pairing problem can be solved. The numerical and experimental mode shapes must be matched. For this purpose, the $MAC_j(\theta)$ ratio is commonly considered. For this purpose, the $MAC_j(\theta)$ ratio among all the numerical and experimental mode shape is computed and organized in a matrix. The rows of this matrix are associated with the numerical mode shapes and the columns with the experimental mode shapes. The component of the matrix with a higher value allows determining the linking among numerical and experimental vibration modes.

Although computational algorithms have been used extensively to cope with this updating problem, they present two clear limitations. First, they elapse a high simulation time when the complexity of the FE model increases. As it is the case of robust FE models. Second, they are not able to deal with uncertainties associated with the experimental modal properties of the system.

To tackle these two issues, a hybrid local–global algorithm combined with a predictive model is used in this paper. In particular, the hybrid Unscented Kalman Filter (UKF)-Harmony Search (HS) algorithm is used to obtain the Pareto front of the bi-optimization problem [19, 23]. This algorithm allows considering the uncertainties of both the measurements and the estimation process and takes advantage of the acceleration scheme provided by the UKF and the global character of the HS. Once the Pareto front is obtained, a decision-making problem must be solved to select the best solution. To cope with this, the Pareto front is processed through a PC analysis and an artificial neural network (ANN) is designed to map the relationship between the physical parameters of the model and the bi-objective function. Finally, the best solution is determined from a local minimization problem. In this sense, the ANN defines a continuous predictive model that allows reducing the number of iterations, thus, the simulation time of the optimization algorithm [20].

In this section, the multi-objective HS, the UKF algorithm and the post-process of the Pareto front are detailed.

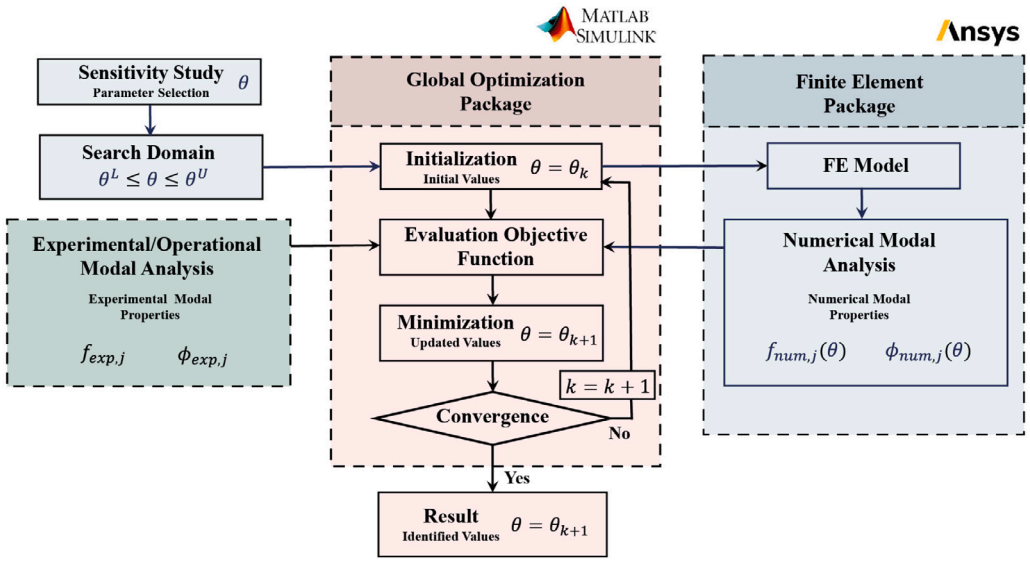

Fig. 1. Flowchart representing the linking between the FE analysis package and the mathematical software for the FE model updating implementation.

2.2. MHS algorithm

The global metaheuristic HS algorithm [24] is inspired in the mental process carried out by musicians when they improvise searching for harmony according to aesthetic requirements. The goal of this algorithm is to find the global minimum of an objective function via the iterative modification of a set of physical parameters of the model. When compared to Genetic Algorithm, the complexity of the mathematical operations implemented in the HS algorithm to monitor the evolution of the population are designed to improve its performance.

The HS algorithm has been implemented successfully for several practical engineering applications [25]. This algorithm has shown a great effectiveness when compared with other conventional metaheuristic algorithms to solve the FE model updating problem of complex civil engineering structures [10].

The HS algorithm consists of the following steps [10]. First, the harmony matrix, H, that stores the initial candidate solutions is created. After that, for each candidate solution the objective function is assessed. The new harmonies are generated using three mechanisms (memory consideration, pitch adjustment and randomization) and the objective function is evaluated again. Finally, the harmony matrix, H, is updated with the best harmonies and the steps are repeated until a convergence criterion is reached.

The MHS is an extension of the above described algorithm which allows minimizing multi-objective functions. When a new harmony is generated, each element of a new candidate vector can be defined in terms of either a previous value stored in the harmony matrix, H, or adopting a new random value. This fact is controlled by the harmony memory consideration rate, HMCR, Thus, for each parameter,a random number, between 0 and 1, is generated and if this number is lower than or equal to *HMCR*, the parameter is chosen randomly from the matrix H. Otherwise, a random value among the possible values of the search domain is assigned to the parameter. Additionally, when some elements adopts the value of a previous one, it can be mutated according to the pitch adjustment rate, *PAR*. This parameter works in the same way as the previous one. In case the parameter must be adjusted, this is based on an additional parameter, the so-called bandwidth, b_w, which is added or subtracted to mutate the considered candidate vector. The classification of the non-dominated solutions is performed using both the non-dominated sorting method and the crowding distance [26]. Finally, in order to restore the initial size of the harmony matrix, H, the worst solutions, according to a crowding distance criterion, are removed. When the convergence criterion is met, the so-called Pareto front is obtained in terms of the non-dominated solutions.

2.3. Unscented Kalman filter

The Unscented Kalman Filter (UKF) is framed within the family of sigma-points Kalman filters [27]. This local algorithm is a derivative free estimator, i.e., no Jacobians or Hessians need to be calculated, broadly employed for nonlinear dynamic systems. The formulation for a parameter estimation problem is represented as [28]:

$$\boldsymbol{\theta}_k = \boldsymbol{\theta}_{k-1} + \mathbf{w}_{k-1} \tag{4}$$

$$\mathbf{z}_k = h(\boldsymbol{\theta}_k) + \mathbf{v}_k \tag{5}$$

being θ the parameter vector; h the nonlinear modelling function, $\mathbf{z}$ the outputs of the dynamic system; $\mathbf{w}$ the statistical noise of the identification process; and $\mathbf{v}$ the statistical noise of observation process. Both type of noise are assumed to be uncorrelated and white Gaussian noise with zero-mean and covariance matrices $\boldsymbol{Q}$ and $\boldsymbol{R}$ respectively. The matrix $\boldsymbol{R}$ may be computed by means of two terms [29]: (i) the measurement noise; and (ii) the modelling noise. If the same FE model is considered for each step, the first component of the matrix $\boldsymbol{R}$ can be neglected [16].

This algorithm performs the nonlinear estimation through the definition of $2n + 1$ (being n the number of parameters) deterministic sampling points (sigma points). Their propagation through the nonlinear function, h, leads to the true posterior mean and covariance of the estimated parameters up to the second order of the Taylor series expansion of the nonlinear function (third order of the Taylor series expansion for a Gaussian inputs). Hence, it is an extension of the unscented transformation [30]. The main computational effort of this algorithm is the computation of the new sigma points which is based on the square-root decomposition of the posterior covariance matrix, $\mathbf{P}$. Thus, this matrix must be positive semidefinite at each step. To employ the Cholesky factorization ($\mathbf{A} = \sqrt{\mathbf{P}} = chol(\mathbf{P})$ being $\mathbf{P} = \mathbf{A}\mathbf{A}^T$) may provide an efficient decomposition but the matrix $\mathbf{P}$ needs to be updated at each iteration and numerical errors can give a non-positive semidefinite matrix. To overcome this issue, the square-root UKF [31] propagates directly the matrix A avoiding the factorization and ensuring that the matrix is positive semi-definite. These sigma points and their associated weights are calculated as:

$$(\chi_{k-1})_0 = \hat{\theta}_{k-1|k-1} \tag{6}$$

$$(\chi_{k-1})_i = \hat{\theta}_{k-1|k-1} + \sqrt{(n+\lambda)}(\mathbf{A}^{\theta}_{k-1|k-1})_i \qquad i = 1, 2, \ldots, n \tag{7}$$

$$(\chi_{k-1})_{i+n} = \hat{\theta}_{k-1|k-1} - \sqrt{(n+\lambda)}(\mathbf{A}^{\theta}_{k-1|k-1})_i \qquad i = 1, 2, \dots, n \tag{8}$$

$$W_0 = \frac{\lambda}{n+\lambda} \tag{9}$$

$$W_i = W_{i+n} = \frac{1}{2(n_d+\lambda)} \qquad i = 1, 2, \dots, n \tag{10}$$

where $\hat{\theta}_{k-1|k-1}$ are the posterior parameters estimated at the previous step and λ is a scaling parameter.

As an algorithm belonging to the Kalman Filter family, the square-root UKF has also two steps: prediction and correction. The former considers the prior model to assess the sigma points, predict the estimation error covariance, $\mathbf{A}^{\theta}$, the model outputs error covariance, $\mathbf{S}^{z}$, and the cross covariance between the estimation error and the model outputs error covariances, $\mathbf{P}^{\theta z}$.

The estimation error covariance is given by $\mathbf{A}^{\theta}_{k} = \gamma^{-1/2}\mathbf{A}^{\theta}_{k-1}$, where γ is a scalar factor slightly less than the unit [31]. Since $W_i > 0$ for all $i \geq 1$, the model output error covariance, $\mathbf{S}^{\mathbf{z}}$, can be expressed as [32]:

$$\begin{aligned}\mathbf{S}^{\mathbf{z}}_{k} = &\sum_{0}^{2n_d} W_i[[(z^{i}_{k|k-1} - \hat{\mathbf{z}}_{k|k-1})] \cdot (z^{i}_{k|k-1} - \hat{\mathbf{z}}_{k|k-1})^{T}] + \mathbf{R} \\ &= [\sqrt{W_i}(z^{i}_{k|k-1} - \hat{\mathbf{z}}_{k|k-1}), \sqrt{\mathbf{R}}] \\ &\cdot [\sqrt{W_i}(z^{i}_{k|k-1} - \hat{\mathbf{z}}_{k|k-1})^{T}, \sqrt{\mathbf{R}}^{T}]^{T} \\ &+ W_0[(z^{0}_{k|k-1} - \hat{\mathbf{z}}_{k|k-1}) \cdot (z^{0}_{k|k-1} - \hat{\mathbf{z}}_{k|k-1})^{T}] \qquad for \quad i = 1 : (n_d)\end{aligned} \tag{11}$$

The first term can be expressed by means of a QR factorization. The last term, can be taken into account performing a rank 1 update to Cholesky factorization. The cross covariance is then calculated as:

$$\mathbf{P}^{\theta \mathbf{z}}_{k|k-1} = \sum_{0}^{2n_d} \left(W_i[(\chi_{k-1})_i - \hat{\theta}_{k|k-1}] \cdot [(z_{k|k-1})_i - \hat{\mathbf{z}}_{k|k-1}]^{T} \right) \tag{12}$$

Finally, the correction step uses both the measurements, $\mathbf{z}^{obs}$, and the model outputs to determine the posterior mean and covariance of the parameter estimation by considering the Kalman"s gain matrix, $\mathbf{K}$.

$$\mathbf{K}_k = (\mathbf{P}^{\theta \mathbf{z}}_{k|k-1} / {\mathbf{S}^{\mathbf{z}}_{k|k-1}}^{T}) / \mathbf{S}^{\mathbf{z}}_{k|k-1} \tag{13}$$

$$\hat{\theta}_{k|k} = \hat{\theta}_{k|k-1} + \mathbf{K}_k(\mathbf{z}^{obs} - \hat{\mathbf{z}}_{k|k-1}) \tag{14}$$

2.4. Post-process of the pareto front

The Pareto front is projected from the functional space to the principal component (PC) space by performing a principal component analysis (PCA) of the constituent points. PCA is a statistical tool to extract patterns from correlated variables following the next steps [33]: first, the data are normalized and their covariance matrix is computed; subsequently, the eigenvalues and eigenvectors of this matrix are calculated, and finally, the PC scores are determined. It is worth pointing out that the eigenvector associated to the highest eigenvalue is the first PC and so on and that the scores represent the projection of the data in the PC space. The resulting Pareto front exhibits a clear convex character which eases the determination of the best solution among all the possible ones as this is addressed solving a local minimization problem.

The approximation of the previous Pareto front to a continuous predictive model is achieved employing an artificial neural network (ANN). This is a supervised machine learning technique that maps nonlinear and coupled relationships between a set of inputs and outputs. The multilayer perceptron (MLP) is the most widely used network topology and consists of an input layer, an output layer and one or several hidden layers, which are interconnected in a feed-forward manner: one neuron sends information to the subsequent layer but does not receive from them. The number of hidden layer can be assumed to be equal to one as it has been demonstrated that only a single hidden layer may approximate any continuous function [34,35]. A trial and error procedure or empirical relationships may me employed to determine the number of neurons. The application of the ANN to the Pareto front allows mapping the relationship between the physical parameters of the model and the multi-objective function playing the role of a convex function. The relationship needs to be trained and tested on the basis of a backpropagation training algorithm that adjusts the weights among the neurons' connection by minimizing the error between the estimated output and the desired output propagated in a backward direction [36].

Taking advantage of the convex character of the continuous function, the decision-making problem to obtain the best solution is transformed into a local minimization problem due to its convergence speed and good accuracy. The solution obtained is the knee-point of the original Pareto front. As local optimization algorithm, the Active-Set (A-S) is hereby adopted [37]. Under this approach, the decision-making problem may be formulated as:

$$\text{minimize} g(\theta) = y(\theta) \tag{15}$$

$$\text{Subjectedto}: \begin{cases} \theta_l \leq \theta \leq \theta_u \\ x(\theta) \geq x_{min} \\ y(\theta) \geq y_{min} \end{cases} \tag{16}$$

being $g(\theta)$ the objective function, θ_l and θ_u are respectively the minimum and maximum values of the physical parameters which form the Pareto front, $(x(\theta), y(\theta))$ are the ANN outputs in the PC space, and x_{min} and y_{min} are the minimum values of the ANN outputs in the PC space.

2.5. Proposed algorithm

The implemented algorithm combines the main virtues of the two described algorithms (MHS and UKF) and the techniques employed to post-process the Pareto front. First, the uncertainties are considered and, second, the computational cost is reduced due two reasons. The first one is the acceleration scheme of the hybrid algorithm itself. The second one lies in the ANN which allows reducing the iterations and the population to obtain a non-crowded Pareto front as this is then simulated by the ANN. Finally, the PCA improves the efficiency of the decision-making problem since it provides a convex representation of the Pareto front which is further employed by the A-S algorithm to obtain the best solution in a straightforward manner (Fig. 2).

3. Validation example: FE model updating of a laboratory footbridge

A real laboratory footbridge is considered as benchmark structure to validate the proposed hybrid-collaborative algorithm. Section 3.1 describes the geometry and main constitutive elements of the structure. Section 3.2 introduces the initial FE model of the footbridge. Then, Section 3.3 presents the dynamic characterization of this structure via a forced vibration test (FVT) together with an EMA algorithm. Subsequently, Section 3.4 details the parameter selection of for the updating process. Finally, Section 3.5 describes in detail the updating process under the maximum likelihood method.

3.1. Geometrical configuration

This benchmark structure is a reconfigurable steel footbridge from the Vibration Engineering Section of the University of Exeter (Fig. 3). The footbridge is a frame structure with a length of 15 m. The structure is comprised of two lateral steel beams separated transversally 2.5 m. Rectangular plates of 200 × 12 mm spaced 1.25 m brace these two beams. Steel bolts connect the deck, made of composite SPS panels [38], with both the longitudinal beams and transversal plates. Four columns directly pinned to the ground are used as support of the four ends of the steel beams. Further information about this footbridge can be found in Ref. [39].

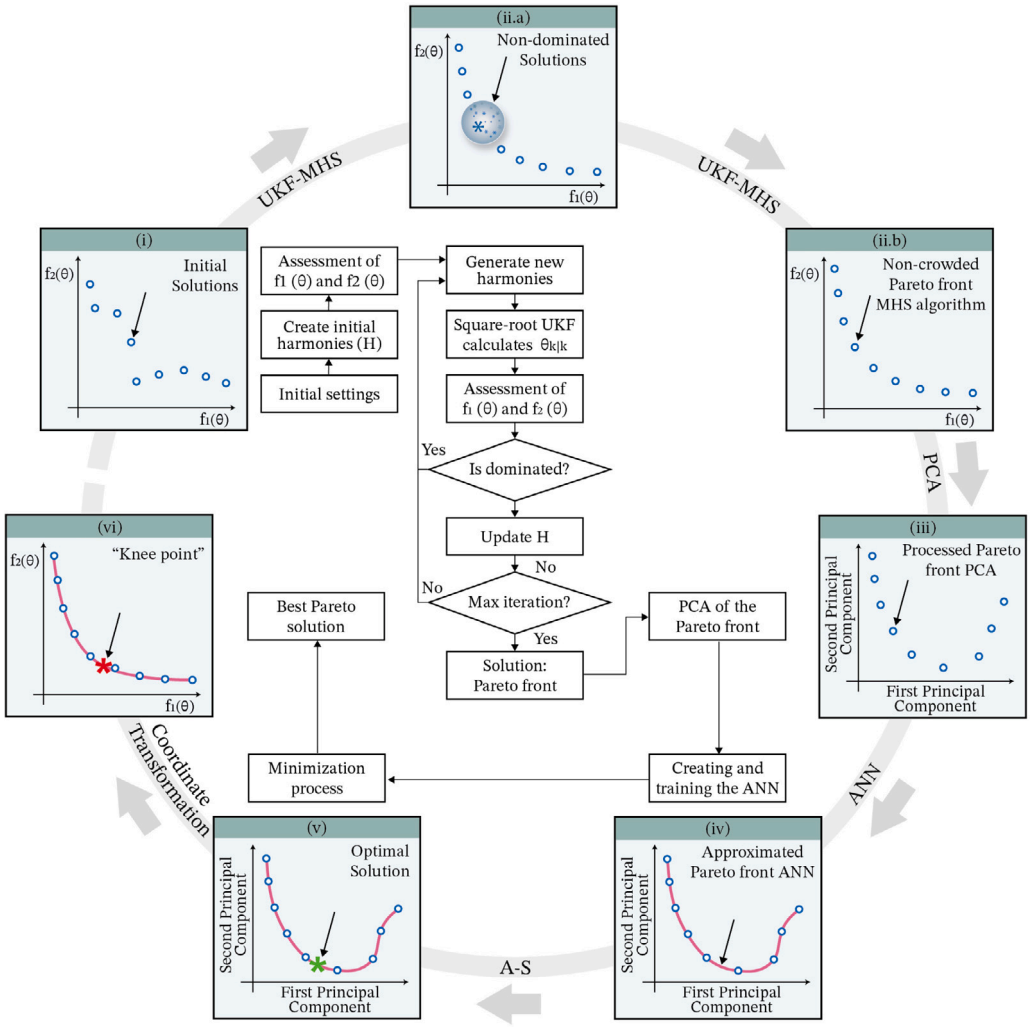

Fig. 2. Flowchart of the proposed combinative computational algorithm.

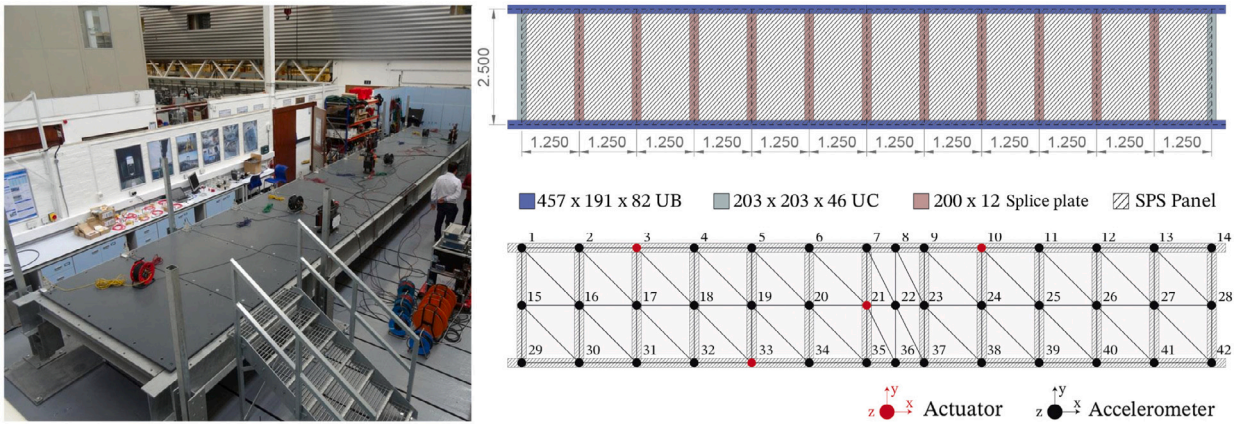

Fig. 3. Description of the laboratory footbridge and layout of the FVT.

3.2. Initial FE model

An initial FE model of the footbridge was built using the Ansys Software [40]. To model the structure, three different types of elements were employed: (i) shell elements (SHELL181) for the lateral beams; the transversal beams and the SPS panel; (ii) 3D beam elements (BEAM188) for the bolts of the connection between the SPS panel and the steel structure; and (iii) equivalent spring element (COMBIN14) with longitudinal and transversal stiffness to model each support whose vertical displacement was constrained. The value of the stiffness at each direction was estimated from a simplified FE model of just the column, resulting in an equivalent stiffness of $5.5 \cdot 10^7$ N/m and $1.0 \cdot 10^7$ N/m for the longitudinal and transversal direction, respectively. The mesh consisted of 31 903 elements. The adopted mechanical properties for

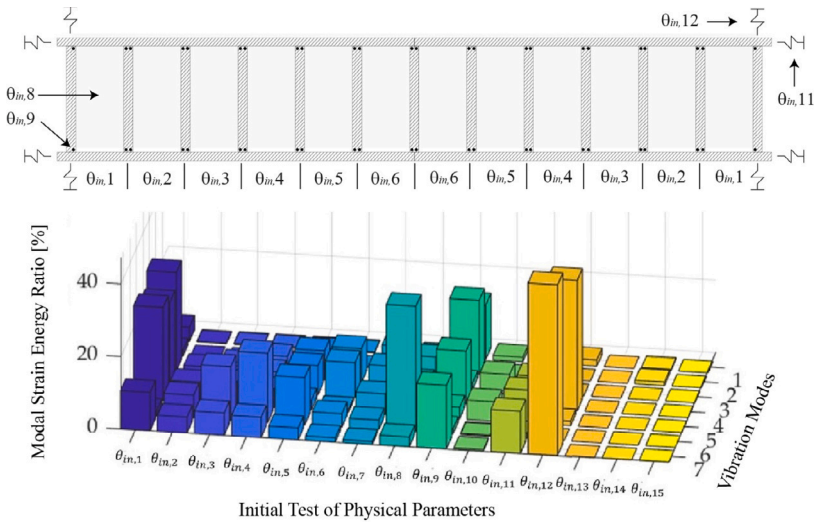

Fig. 4. Sensitivity study to select the most relevant physical parameters of the footbridge model.

Table 1
Experimental natural frequency, f_{exp} , initial numerical natural frequency f_{ini}, relative difference, $\triangle f$, and the MAC ratio.

Vibration mode	f_{exp} [Hz]	f_{ini} [Hz]	$\triangle f$ [%]	MAC [-]
1	3.810	3.638	−4.51	0.998
2	5.144	5.433	5.62	0.994
3	8.485	9.106	7.32	0.988
4	12.366	11.310	−8.54	0.877
5	18.605	17.364	−6.67	0.985
6	20.459	19.519	−4.59	0.993
7	22.980	20.725	−9.81	0.634

the different materials are the followings: (i) for the steel, a density of$\rho_s = 7850\ \text{kg/m}^3$, the Young's modulus equals $E_s = 210 \cdot 10^9$ Pa and a Poisson's ratio of $\upsilon_s = 0.3$; and (ii) for the polyurethane the density was assumed to be $\rho_p = 1100\ \text{kg/m}^3$, the Young's modulus $E_p = 7.5 \cdot 10^8$ Pa and the Poisson's ratio $\upsilon_p = 0.3$.

The numerical modal analysis of this model gives as result the seven natural frequencies shown in Table 1 and the mode shapes depicted in Fig. 5.

3.3. FVT and EMA

The experimental modal identification of the footbridge was carried out through the experimental modal analysis of the accelerations recorded in a forced vibration test. To do this, a set of proof-mass actuators and accelerometers were employed (Fig. 3).

Random signals were used as input to simultaneously drive the actuators within a Multiple Input-Multiple Output (MIMO) configuration [41]. From the applied forces and accelerations response, the Frequency Response Function was calculated considering an overlap of 50%. After this, a complex mode indicator function was defined to identify probable mode location in the FRFs fitted curves. To finish the process, a global polynomial curve fitting method extracts the first seven experimental natural frequencies given in Table 1 and their mode shapes (shown in Fig. 5) from the abovementioned probable mode locations. The reader can refer to Ref. [39] for further explanation regarding the forced vibration test and the experimental modal analysis.

3.4. Parameters selection and search domain of the FE model updating process

Based on the differences between the numerical and experimental modal properties, the FE model of the footbridge is updated applying the proposed algorithm. Firstly, the physical parameters of the model that are being updated must be identified. The ratio between the modal strain energy associated with each parameter and the overall modal strain energy is considered as criterion to reveal the influence of the parameter on the variation of the natural frequencies [42]. Thus, the parameters with greater ratios are selected. An initial set of 15 physical parameters were taken into account in this analysis and, as result, ten were selected as design parameters (designated as in Fig. 4): Young's modulus of the steel of the longitudinal beams at 6 different sections ($\theta_{in,}1 - \theta_{in,}6$), Young's modulus of the polyurethane ($\theta_{in,}8$), Young's modulus of the steel of the bolts ($\theta_{in,}9$), equivalent longitudinal stiffness of the supports ($\theta_{in,}11$) and the equivalent transversal stiffness of the supports ($\theta_{in,}12$). The selection of the Young's modulus of the different material as physical parameter has not got as objective the identification of this structural property via the resolution of the inverse problem. However, this magnitude is used as estimator of the stiffness of the structure. In this manner, the variation of this quantity with respect to its reference value reflects the reduction of some uncertainties (geometrical tolerances, constitutive laws ...) associated with the modelling of the structure.

In addition, a search domain has been established for each design parameter in order to constrain the optimization problem and to guarantee an adequate physical meaning of the updated value. The considered research domain for each considered updating parameter with its lower and upper bound is illustrated by Table 2. Once both the design parameters and their search range have been set, the FE model updating process is performed.

3.5. FE model updating process

The previous described bi-objective algorithm is applied for the model updating of the footbridge. The followings values for the parameters of the MHS algorithm were adopted [22,43]: a HMCR ratio of 0.9, a PAR ratio of 0.7 and a bandwidth, b_w, equals the 1% of the search domain of each parameter. Regarding the parameters of the UKF algorithm, the sensitivity analysis carried out by the authors in Ref. [19] was used, thus, the values of the parameters were: number of iterations of the UKF algorithm, NUKF=3, initial estimation error covariance, $P_0^{\theta} = diag(((\theta_u - \theta_l)/2000)^2)$ and measurement noise covariance matrix, $R_{ii} = 0.001$. The number of iterations of the MHS algorithm was set to 10, the number of initial harmonies was 20 and the number of new harmonies, generated at each iteration, equals 5. As result, the non-crowded Pareto front containing the possible solutions was obtained (see Fig. 6a). The computational cost of this step of the

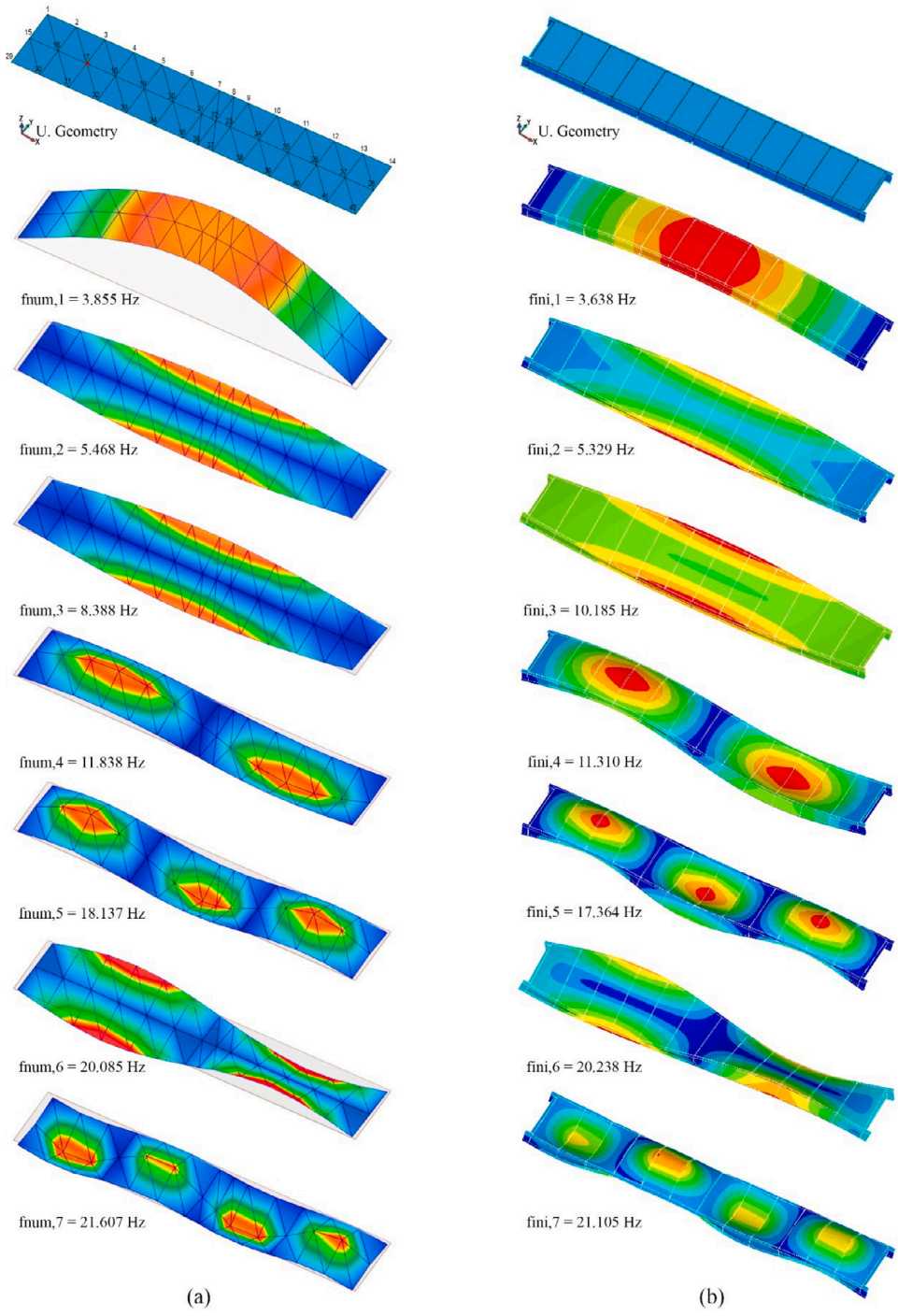

Fig. 5. First seven mode shapes obtained from: (a) the experimental identification test; and (b) the initial FE model.

proposed algorithm is the highest, as it took 4678 s to obtain the non-crowded Pareto front.

Next, the PCA analysis of this Pareto front is conducted according to the steps of the proposed algorithm. The singular value decomposition method was employed to perform the decomposition of the covariance matrix. Fig. 6b shows the projection of the Pareto front in the PC space. As mentioned in Section 2, this analysis presents two advantages. Firstly, the accuracy of the ANN used in the next step to approximate the Pareto front is improved and, secondly, the selection of the best solution is more robust due to the convex nature of the Pareto front in the PC space. The time to perform this analysis is negligible when compared to the bi-objective optimization as it takes less than one second.

The fourth step of the algorithm involved the design of the ANN to approximate the Pareto front. The objective is to simulate the relationship between the ten physical parameters and the two residuals of the bi-objective function in a continuous manner, yielding a continuous Pareto front which leads to a simpler decision-making problem. In this study the MLP (Multi-layer perceptron) with one hidden layer has been used as ANN topology. The rule of Kermanshahi [44] allows calculating the number of neurons of the hidden layer as neurons $= (m+n)/2+\delta$, being m and n the number of neurons of the input and output layers, respectively, and δ a normalization factor which can be equal to 1 or 2. Thus, for this case $m = 10$, $n = 2$ and $\delta = 1$, giving as result 7 neurons for the hidden layer. The ANN was trained using the Levenberg–Marquardt backpropagation algorithm [36], defining the error function in terms

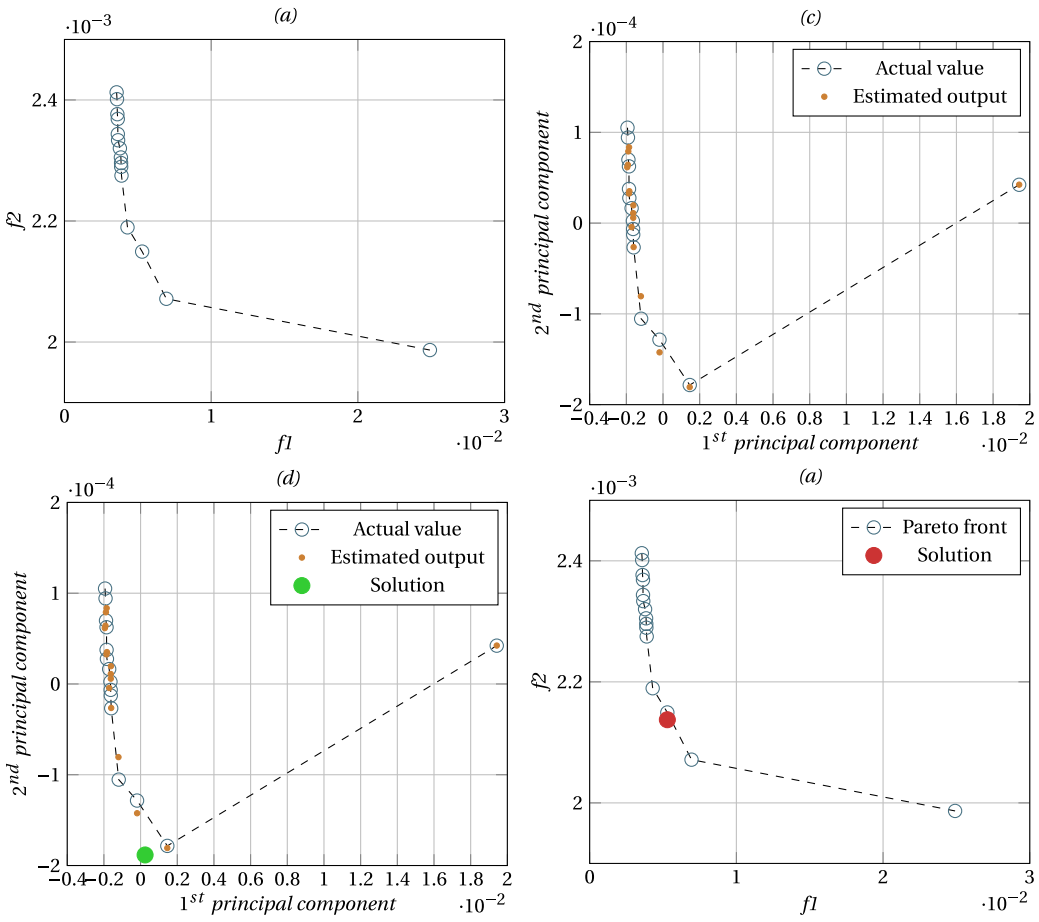

Fig. 6. Combinative computational algorithm: (a) non-crowded Pareto front, (b) PCA analysis, (c) solution using the ANN and (d) corresponding solution in the original Pareto front.

Table 2
Updated value of the physical parameters of model, θ_{in}, after the updating process.

Parameter	Description		Initial value	Range of variation		Updated value
				Lower	Upper	
$\theta_{in}, 1$	E_s long. beam section 1	[GPa]	210	190	240	230.08
$\theta_{in}, 2$	E_s long. beam section 2	[GPa]	210	190	240	215.94
$\theta_{in}, 3$	E_s long. beam section 3	[GPa]	210	190	240	202.43
$\theta_{in}, 4$	E_s long. beam section 4	[GPa]	210	190	240	215.92
$\theta_{in}, 5$	E_s long. beam section 5	[GPa]	210	190	240	193.52
$\theta_{in}, 6$	E_s long. beam section 6	[GPa]	210	190	240	214.58
$\theta_{in}, 8$	E_p polyurethane	[MPa]	1000	500	1500	758.92
$\theta_{in}, 9$	E_s steel bolts	[GPa]	1000	210	2100	790.95
$\theta_{in}, 11$	K Equivalent long. stiffness	[N/m^2]	$6.0 \cdot 10^7$	$1.4 \cdot 10^7$	$1.1 \cdot 10^8$	$7.06 \cdot 10^7$
$\theta_{in}, 12$	K Equivalent transv. stiffness	[N/m^2]	$9.0 \cdot 10^6$	$4.8 \cdot 10^6$	$3.8 \cdot 10^7$	$7.79 \cdot 10^6$

of the mean square error and considering 70% of the elements of the Pareto front for sampling. The rest of the elements were used to validate and test the ANN. Fig. 6b illustrates the accuracy of the ANN used to continuously approximate the Pareto front in the PC space.

Finally, the decision-making problem is solved to obtain the best solution (knee point). For this purpose, the A-S algorithm has been used to conduct the minimization problem. Once this point is obtained, it is projected back into the original Pareto front (Fig. 6c-d). The simulation time to design the ANN and calculate the knee point was about 5 s. The physical parameters associated to this optimum point (updated values) are collected in Table 2 and the corresponding modal properties of the updated FE model are shown in Table 3.

It can be observed that after the updating process, all the MAC ratios are above 0.89 and the relative differences have been reduced. In addition, the computational cost to perform this process has been also less than traditional bi-objective optimization as it is not needed a populated Pareto front, and, therefore, the number of iterations and population of the algorithm can be set to low values.

Table 3
Experimental natural frequency, f_{exp} , updated numerical natural frequency f_{upd}, relative difference, $\triangle f$, and the MAC ratio.

Vibration mode	f_{exp} [Hz]	f_{upd} [Hz]	Δf [%]	MAC [-]
1	3.810	3.844	0.892	0.999
2	5.144	5.458	6.104	0.994
3	8.485	8.388	1.143	0.988
4	12.366	11.858	4.107	0.890
5	18.605	18.148	2.456	0.986
6	20.459	20.185	1.339	0.993
7	22.980	21.607	5.975	0.963

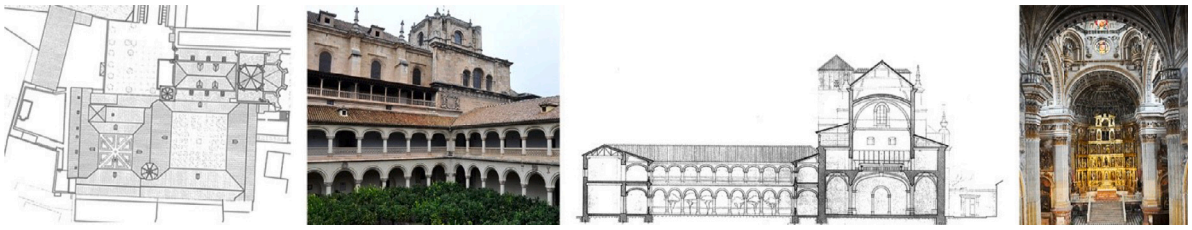

Fig. 7. Royal Monastery of San Jerónimo: (a) General ground floor, (b) Largest cloisters, (c) Cross section, (d) Interior church.

Therefore, Fig. 6 summarizes the different steps of the proposed algorithm. The first step is the determination of the non-crowded Pareto front using the UKF-MHS algorithm. Subsequently, a PCA is performed in order to find the coordinates that minimize the uncertainty of the non-crowded Pareto front. A geometrical transformation is implemented on this Pareto front. Lately, a continuous mapping is established between the updating parameters and the Pareto front using an ANN. The convex form of this ANN allows obtaining its global minimum, the "knee" point", using a gradient-based optimization algorithm (A-S). Finally, after the "knee" point is determined, the same one is depicted in the original function space.

4. Case study: Church of the royal monastery of san jerónimo

This section presents the application of the proposed approach on the Royal Monastery of San Jerónimo (Granada, Spain) with the aim of verifying its validity on this type of historic buildings. Section 4.1 describes the historical context and the architectural configuration of the heritage complex, highlighting the church as a case study. Section 4.2 introduces the initial FE model of the church. Then, Section 4.3 presents the dynamic characterization of the church by means of an ambient vibration test (AVT) together with two OMA algorithms. Finally, Section 4.4 details the updating process of the initial FE model under the bi-objective proposed approach.

4.1. Historical context and architectural configuration

The Royal Monastery of San Jerónimo is part of a larger heritage complex that belongs to the Jerónima order. The construction of the monastery dates from the 16th century and consists of a church and two cloisters, around which the different chambers are distributed (Fig. 7a). The main cloister presents a square shape with two levels. The lower body has thirty-six Gothic arches supported by strong capitals, with a total length of 29 × 29 m. The second cloister also develops through galleries on two levels with different architectural styles (Gothic, Mudejar and Renaissance). In this case the plant has dimensions of 17 × 17 m. The church, which also dates from the 16th century, is attached to the main cloister (Fig. 7b) and located in the northeast area is the church. Initially the style of the complex was Gothic until the work was commissioned to Jacobo Florentino who, along with his successor Diego de Siloe, endowed the temple with its actual Renaissance style.

The church, which a Latin cross plan and a polygonal apse, has non-protruding transepts on the lower floor. At this level, the side chapels are covered with ribbed Gothic vaults (Fig. 7c). The total dimensions of the church floor plan are 57 × 24 m, with a height of 30 m in the central nave and 35 m up to the dome (Fig. 7d). The transept and the apse are covered with barrel vaults. Next to the front of the church is the tower that was finished in 1565. This construction is made up of three parts adding a total of 46 m up to the bell tower [45].

4.2. Initial FE model

The application of the OMA is usually requires the creation of an initial model (Fig. 8) in order to estimate numerically the natural frequencies and mode shapes and thus determine adequate positions of the accelerometers. The FE model of the church was built using Ansys Software [40]. This model is mainly composed of five groups of elements: stone walls and buttresses, brick masonry vaults, concrete floors, and fills. The types of elements used to configure the FEM are: (i) 3D-solid elements (SOLID45) for the fills, (ii) 3D-shell elements (SHELL63) for the rest of the elements; and (iii) 1D-spring elements (COMBIN14) for the boundary conditions. The model contemplates constructive and structural considerations such as: the contact between the church and the main cloister by means of spring elements, the weight of the wooden roof located over the central nave and the weight of the concrete lining walls that reinforce the last section of the tower. The final model comprises 423,627 elements, 91,773 nodes and 469,619 degrees of freedom.

Material properties were initially estimated from the literature [46]. For the stone masonry, in walls and buttresses, the properties adopted were: (i) density, 2100 kg/m^3; (ii) Young's modulus, 2000 MPa; and (iii) Poisson's ratio 0.2. For the brick masonry vaults, the following properties were considered: (i) density, 1800 kg/m^3; (ii) Young's modulus, 2000 MPa; and (iii) Poisson's ratio 0.2. For the concrete floor, the following values were taken into account: (i) density, 2500 kg/m^3; (ii) Young's modulus, 24 000 MPa; and (iii) Poisson's ratio, 0.2. For the fillings, the following data were considered: (i) density, 1600 kg/m^3; (ii) Young's modulus, 500 MPa; and (iii) Poisson's ratio, 0.2. Finally, the springs were defined by a stiffness of 2000 kN/m. Based on the largest modal displacements obtained from this initial numerical model, the most suitable positions were selected to carry out the ambient vibration tests (Fig. 9).

4.3. AVT and OMA

AVT and the OMA method were used to determine the dynamic characteristics of the church of the Real Monastery of San Jerónimo. These tests were carried out between 15-17th July (2020) in order to identify the natural frequencies, the modal shapes and the modal damping ratios of the building.

4.3.1. AVT

The experimental campaign was designed taking into account the results obtained in the modal analyses carried out on the initial FE model. In order to fully cover the area of interest, a network was drawn including a total of 62 points. Fig. 9 details the position of these measurement points. Red points mark the situation of the two reference accelerometers while black points the moving ones. All these points were set in the three principal directions to capture the global mode shapes in the longitudinal, lateral and vertical direction of the complex. Since two of the accelerometers (placed at points 16–44, Fig. 9) were kept fixed for reference, a series of twelve set-ups were necessary to cover all measuring points. In each one of these set-ups, accelerations were recorded with a sampling rate of 100 Hz and a sampling time of 12 min.

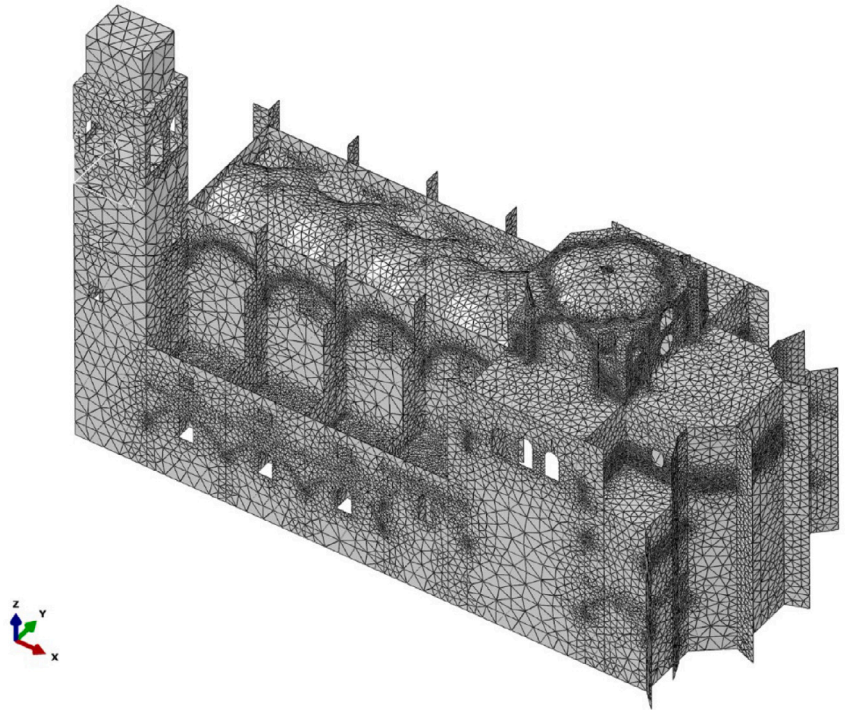

Fig. 8. Initial FE model of the Royal Monastery of San Jerónimo.

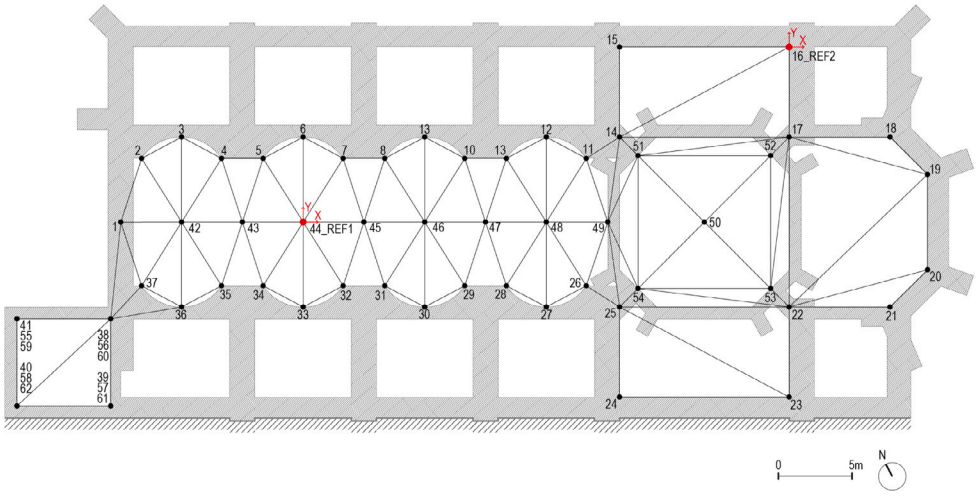

Fig. 9. Accelerometer location and direction.

The equipment used for these tests was composed by eight triaxial force balance accelerometers with a bandwidth ranging from 0.01 to 200 Hz, a dynamic range of 155 dB, a sensitivity of 10 V/g and 1.83 kg of weight (Model ES-T). These accelerometers were connected via three 100-metre long and five 40-metre cables to a thirty-six-channel data acquisition system, provided with anti-alias filters (model OBSIDIAN). The equipment is manufactured by the company KINEMETRICS.

4.3.2. OMA

The data obtained in-situ were processed with the software ARTEMIS [47] using two different identification methods: Enhanced Frequency Domain Decomposition (EFDD) [48] and Stochastic Subspace Identification (SSI-UPCX) [49]. In this way, the mode shapes and the modal frequencies of the gallery were obtained. The resulting modal parameters of the gallery are summarized in Table 4.

As indicated in Table 4, the first four vibration modes of the church have been identified in the frequency range from 0 to 3.5 Hz. Frequency values are obtained with a high degree of reliability, with differences lower than 1.5% between both methods. However, the values of the damping ratios present larger variability. Finally, in relation to the mode shapes, the first mode involves only the tower, the second mode is a transverse translation mode that involves the tower and the transept area, the third is a simple transverse translation mode and the fourth mode corresponds to a bending of the vaults with a turning point in the centre of the central nave. The great complexity of these modes can be seen in Fig. 10a.

4.4. Parameters selection and search domain of the FE model updating process

Based on the experimental results, the initial numerical model was updated to simulate the current modal behaviour of the church following the bi-objective approach proposed in this paper. Firstly, a

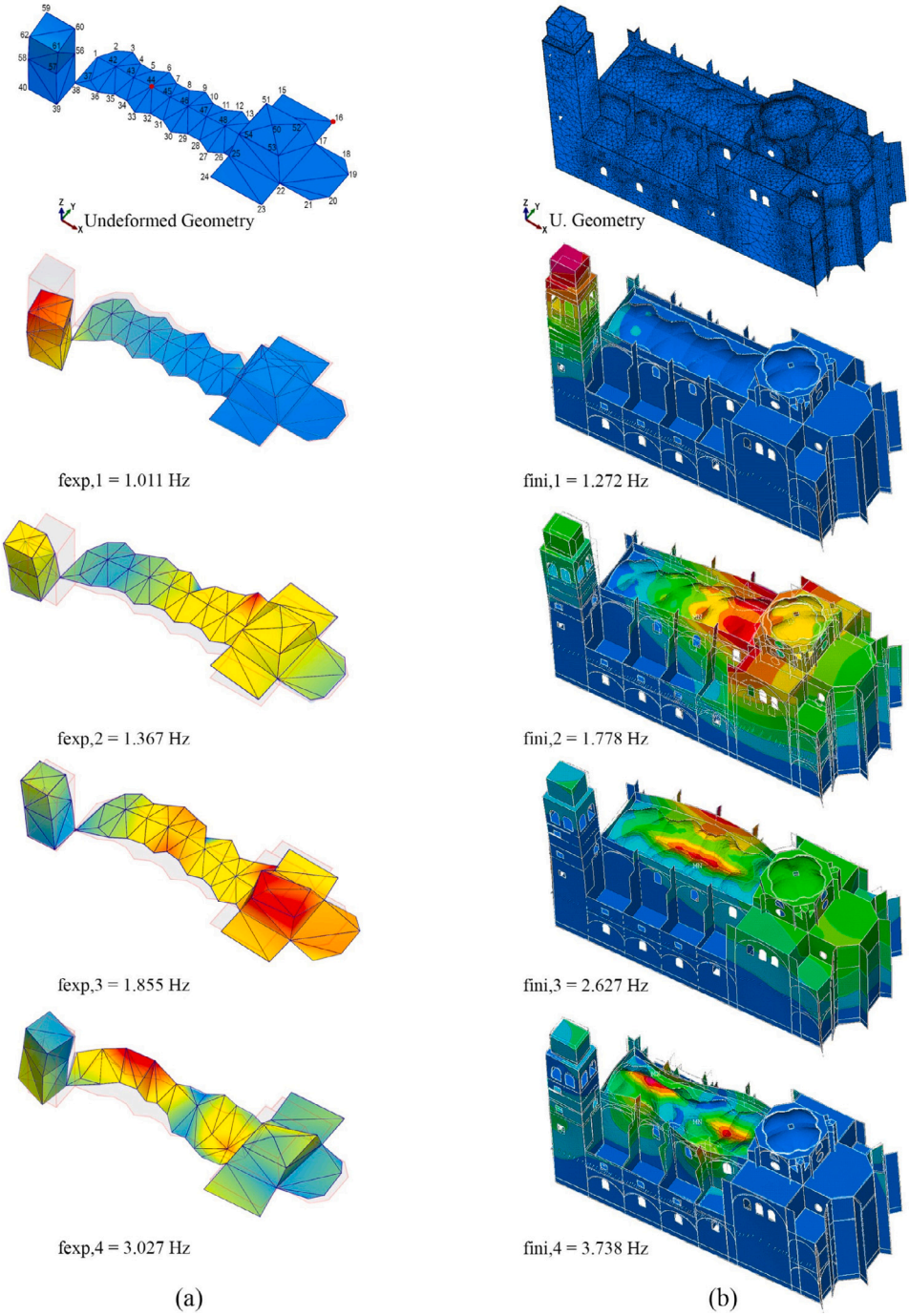

Fig. 10. First four mode shapes obtained from: (a) the experimental identification test; and (b) the initial FE model.

sensitivity study was performed in order to select the most influential physical parameters of the model, θ_{in}. The materials that make up the initial FE model were evaluated with the aim of carrying out a reliable sensitivity study, in this way the 5 groups described above were subdivided into a total of 11 since aspects such as humidity and constructive composition of the different structural elements were considered. For this, the following 11 parameters were initially selected: (i) Young's modulus of the stone, θ_{in}, 1, θ_{in}, 3, θ_{in}, 7 [MPa]; (ii) Young's modulus of brick masonry θ_{in}, 2, θ_{in}, 10 [MPa]; (iii) Young's modulus of wet stone θ_{in}, 4 [MPa]; (iv) equivalent Young's modulus of stone combined with concrete θ_{in}, 5, θ_{in}, 9, θ_{in}, 11 [MPa]; (v) spring stiffness θ_{in}, 6 [kN/m] and (vi) Young's modulus of concrete θ_{in}, 8 [MPa].

The established selection criterion was the modal strain energy that is associated with each parameter. The analysis of this sensitivity matrix shows the value of the relationship between mode shapes and the modal strain energy. Fig. 11 shows the considered physical parameters of the model and the results of the parameter selection process.

The physical parameters to be updated were: (i) the Young's modulus of the stone masonry walls, θ_{in},1; (ii) the brick masonry vaults, θ_{in},2; (iii) the stone masonry buttress, θ_{in},3; (iv) the wet stone masonry

Table 4
OMA results: natural frequencies (Hz), damping ratios (%) and complexity (%).

Mode	EFDD			SSI-UPCX		
	f [Hz]	ξ [%]	Comp. [%]	f [Hz]	ξ [%]	Comp. [%]
1	1.011	0.846	1.260	1.013 (0.29%)	0.632 (25.3%)	1.489
2	1.367	0.970	0.975	1.381 (1.02%)	0.873 (10.0%)	0.888
3	1.855	1.313	3.635	1.852 (0.16%)	1.917 (45.8%)	6.883
4	3.027	1.186	8.939	3.048 (0.69%)	1.745 (47.1%)	27.44

*The percentages in parenthesis correspond to the relative differences between frequencies and damping ratios.

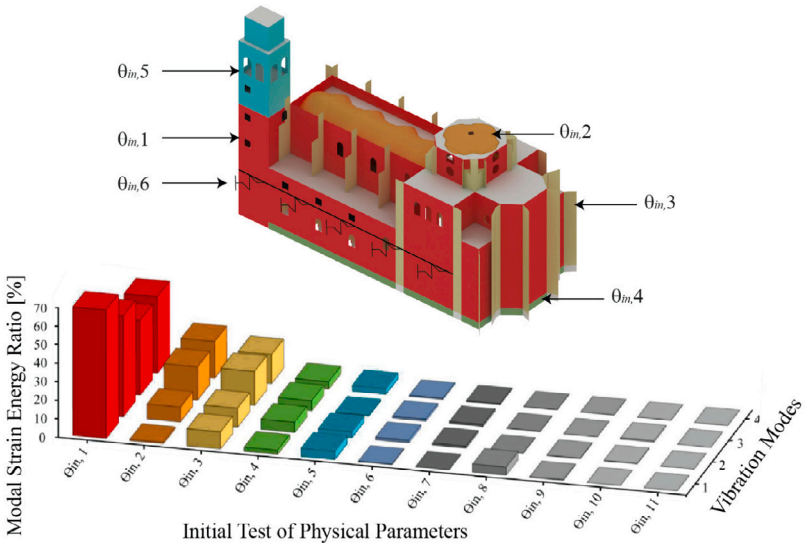

Fig. 11. Sensitivity study to select the most relevant physical parameters of the church model.

walls, θ_{in},4; and (v) the stone combined with concrete walls, θ_{in},5; and (vi) spring stiffness, θ_{in},6. Table 5 shows the initial values and the lower and upper bounds of the design variables. Taking into account the good quality of the experimental data, the four identified modes were selected as target modes in the updating process.

4.5. FE model updating process

Subsequently, the FE model updating process is performed. For this purpose, the followings values for the parameters of the MHS algorithm were adopted: a HMCR ratio of 0.8, a PAR ratio of 0.3 and a bandwidth, b_w, equals the 1% of the search domain of each parameter. Regarding the parameters of the UKF algorithm, the following values were employed: (i) number of iterations of the UKF algorithm, NUKF=3; (ii) initial estimation error covariance, $P_0^{\theta} = diag(((\theta_u - \theta_l)/2000)^2)$; and (iii) measurement noise covariance matrix, $R_{ii} = 0.001$. The number of iterations of the MHS algorithm was set to 40, the number of initial harmonies was 50 and the number of new harmonies, generated at each iteration, equals 25. As result, the non-crowded Pareto front containing the possible solutions was obtained (see Fig. 12a). The computational cost of this step of the proposed algorithm is the highest, as it took 44 h to obtain the non-crowded Pareto front. Fig. 12b shows the projection of the Pareto front in the PC space. The design of the ANN was conducted employing the same rules of the previous section. For this case, the number of neurons of the hidden layer is equal to 4. After the training with the Levenberg–Marquardt backpropagation algorithm, the ANN simulated the Pareto front in the PC space giving as result the estimated outputs depicted in Fig. 12b. The solution of the decision-making problem is represented in Fig. 12c and Fig. 12d after its projection into the original Pareto front space. The updated values of the physical parameters are shown in Table 5.

Table 6 summarizes the results after the updating process and confirms the high correspondence of the results between the calibrated model and those obtained from ambient vibration tests. It can be noted that the updated frequencies are close to the experimental ones, differing by less than 7% while exhibiting MAC values in a range from 0.760 (mode 4) to 0.977 (mode 1) for the four considered mode shapes. Fig. 10 confirms the high correspondence between the mode shapes of the experimental identification process and the FE model. Considering the FE model employed in this section, the computational cost, used to calibrate it, is low as the elapsed time was about 45 h.

Finally, the main advantages of the proposed combinative computational algorithm in comparison with the conventional bi-objective optimization method are remarked in Fig. 12. A clear reduction of the computational time due to the use of a local–global optimization (UKF-MHS) algorithm together with the computation of a non-crowded Pareto front is highlighted. Additionally, a direct estimation of the "knee point", inside the curve generated by the Pareto front, is achieved by the combination of the different statistical learning techniques. In this manner, this proposal allows reducing the requited simulation time without compromising the accuracy of the solution.

5. Conclusions

In this manuscript a combinative computational algorithm is proposed to improve the robustness of FE model updating of complex historical constructions. The proposal takes advantage of the main strengths of two previous algorithms proposed by the authors in order to obtain a new powerful numerical tool which can assist architects and structural engineers in the model updating of complex historical structures. The combinative work, performed between the two primitive algorithms, allows that the global performance achieved by this

Table 5
Updated value of the physical parameters of model, θ_{in}, after the updating process.

Parameter	Description		Initial value	Range of variation		Updated value
				Lower	Upper	
$\theta_{in,}1$	E stone masonry walls	[MPa]	2000	500	3000	1101
$\theta_{in,}2$	E brick masonry vaults	[MPa]	2000	500	3000	1071
$\theta_{in,}3$	E stone masonry buttress	[MPa]	2000	500	3000	598
$\theta_{in,}4$	E wet stone masonry walls	[MPa]	1500	500	3000	509
$\theta_{in,}5$	E stone concrete walls	[MPa]	24 000	14 000	34 000	23 717
$\theta_{in,}6$	K spring stiffness	[kN/m]	2000	1000	3000	1507

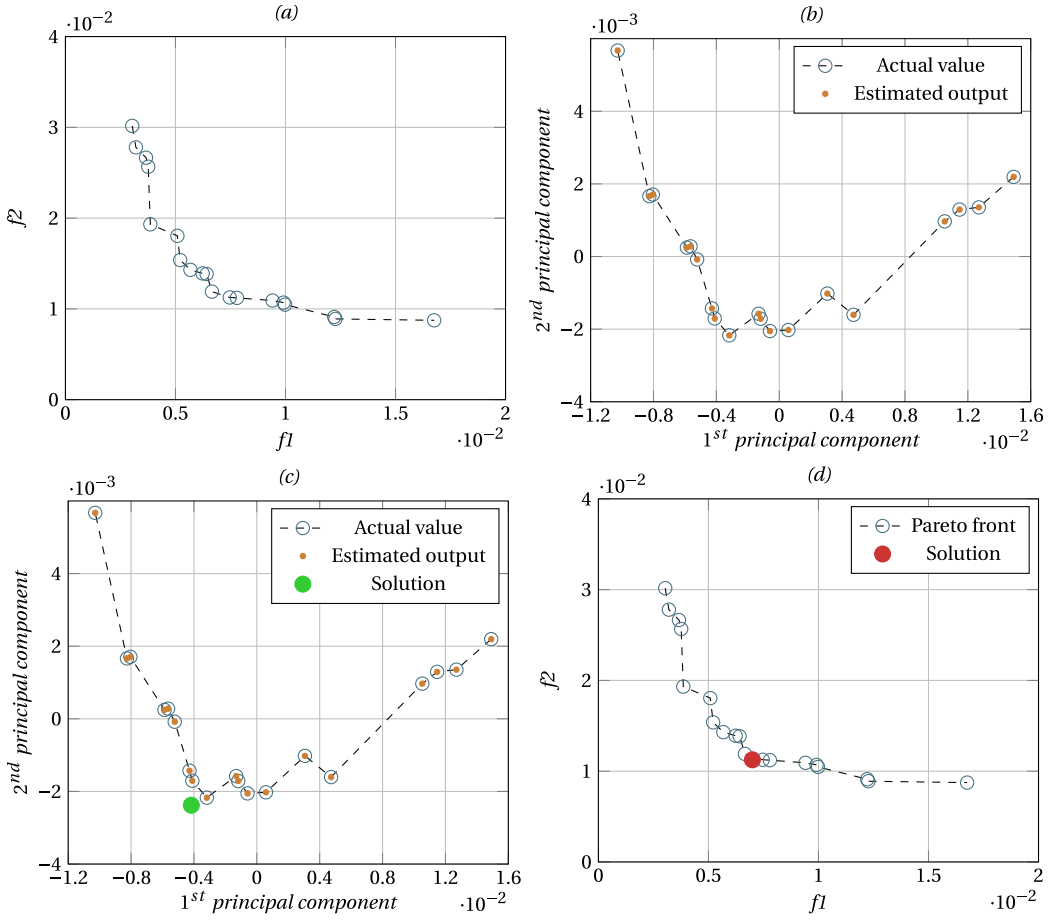

Fig. 12. Collaborative computational algorithm: (a) non-crowded Pareto front, (b) PCA analysis, (c) solution using the ANN and (d) corresponding solution in the original Pareto front.

Table 6
Experimental natural frequency, $f_{exp,j}^{EFDD}$; initial numerical natural frequency, $f_{ini,j}$; relative initial difference, $\triangle f_{exp,j}^{ini,j}$; the initial $MAC_{exp,j}^{ini,j}$ ratios; the updated natural frequency, $f_{upd,j}$; the relative updated difference, $\triangle f_{exp,j}^{upd,j}$; and the updated $MAC_{exp,j}^{upd,j}$ ratios for each considered mode shapes j after the updating process considering the bi-objective approach.

Mode	$f_{exp,j}^{EFDD}$	Initial			UKF-MHS		
	[Hz]	$f_{ini,j}$ [Hz]	$\triangle f_{exp,j}^{ini,j}$ [%]	$MAC_{exp,j}^{ini,j}$ [-]	$f_{upd,j}$ [Hz]	$\triangle f_{exp,j}^{upd,j}$ [%]	$MAC_{exp,j}^{upd,j}$ [–]
1	1.011	1.272	25.82	0.966	0.945	6.53	0.977
2	1.367	1.778	30.07	0.944	1.339	2.05	0.974
3	1.855	2.627	41.62	0.926	1.983	6.90	0.930
4	3.027	3.738	23.49	0.633	2.819	6.87	0.760

proposal was greater than the sum of the local performance of each preliminary algorithm.

As for practical FE model updating, the problem is usually formulated according to the maximum likelihood method, this approach has been considered as basis for the formulation of the updating problem. Thus, the updating problem can be transformed into two sub-problems: (i) a bi-objective optimization sub-problem and (ii) a decision-making sub-problem. The maximum likelihood method presents two clear advantages, when it is implemented to cope with this problem, an easy implementation and understandable interpretation of the updating results. However, there is a clear limitation when this approach is applied for the FE model updating of complex historical construction, the high simulation required to solve the updating problem.

In order to shed some light to this problem, a new combinative computational algorithm has been proposed herein. Three are the main objectives of this proposal: (i) to reduce the computational time requited to solve the FE model updating problem; (ii) to guarantee an adequate accuracy of the solution obtained; and (iii) a direct solution of the updating problem without the necessity of solving different sub-problems.

For this purpose, the proposed algorithm combines the strength of two previously proposed algorithms: (i) a local–global (UKF-MHS) optimization algorithm, which allows increasing the computational

speed of the searching process together with a better quantification of the uncertainty associated with the variability of the experimental measurements; and (ii) a collaborative algorithm in which several statistical learning techniques are linked to make easier the determination of the "knee" point among the different elements of the Pareto front.

Therefore, the main contribution of this manuscript is not only the combination of both algorithms in order to obtain a new proposal with higher performance than the two primitive algorithms but also the implementation of this proposal for the FE model updating of a complex historical construction.

In order to clarity the implementation of the algorithm, two different numerical applications have been included herein: (i) a validation examples, in which the proposed algorithm has been described in detail when it is implemented for the FE model updating of a laboratory footbridge; and (ii) a case study, in which the performance of the proposed algorithm has been assessed when it is implemented for the FE model updating of a complex historical construction. The good performance of the proposal has been highlighted not only in the non-crowded Pareto front computed to solve the problem (with a clear reduction of the computational time) but also for the good accuracy of the "knee" point obtained (inside the curve that defines the Pareto front).

Despite the good results obtained, further studies are needed to assess the performance of this proposal when it is subjected to different updating scenarios. In this sense, it is interesting the analysis of the efficiency of this combinative algorithm either when a regularization term is included in the definition of the objective function (to guarantee the stability of the solution when the number of updating parameters is greater than the number of identified modal properties) or when a meta-model, based on some subrogate modelling technique, is "on-line" updated to assist in damage detection applications for civil engineering structures considering a structural health monitoring strategy.

CRediT authorship contribution statement

Javier Naranjo-Pérez: Writing – original draft, Visualization, Validation, Investigation, Formal analysis, Conceptualization. **Rubén Rodríguez-Romero:** Writing – original draft, Visualization, Validation, Investigation, Formal analysis. **Pablo Pachón:** Writing – review & editing, Writing – original draft, Visualization, Validation, Methodology, Investigation, Formal analysis. **Víctor Compán:** Resources, Project administration, Methodology, Funding acquisition, Data curation. **Andrés Sáez:** Supervision, Methodology, Funding acquisition, Conceptualization. **Aleksandar Pavic:** Resources, Project administration, Methodology, Data curation. **Javier Fernando Jiménez-Alonso:** Writing – review & editing, Writing – original draft, Validation, Supervision, Methodology, Investigation, Conceptualization.

Declaration of competing interest

The authors declare that they have no known competing financial interests or personal relationships that could have appeared to influence the work reported in this paper.

Data availability

Data will be made available on request.

Acknowledgements

This research was funded by two research projects: (i) grant number US-1381164 by the Andalusian Regional Government (Spain); and (ii) "Transport Infrastructures subjected to dynamic loading: assessment techniques for the sustainability, intelligent maintenance and comfort", grant number PID2021-127627OB-I00 and 10.13039/501100011033 by Ministerio de Ciencia e Innovación, Spain, Agencia Estatal de Investigación, Spain and FEDER, European Union.

References

[1] Betti M, Vignoli A. Modelling and analysis of a romanesque church under earthquake loading: Assessment of seismic resistance. Eng Struct 2008;30(2):352–67. http://dx.doi.org/10.1016/j.engstruct.2007.03.027.

[2] Spinelli P, Salvatori L, Lancellotta R, Betti M. Preliminary assessment of the seismic behaviour of giotto's bell tower in florence. Int J Archit Herit 2022;17:23–45.

[3] Standoli G, Salachoris GP, Masciotta M, Clementi F. Modal-based femodel updating via genetic algorithms: exploiting artificial intelligence to build realistic numericalmodels of historical structures. Constr Build Mater 2021;303. http://dx.doi.org/10.1016/j.conbuildmat.2021.124393.

[4] Atamturktur S, Hemez F, Laman J. Uncertainty quantification in model verification and validation as applied to large scale historic masonry monuments. Eng Struct 2012;43:221–34. http://dx.doi.org/10.1016/j.engstruct.2012.05.027.

[5] E.Mottershead J, Link M, Friswell MI. The sensitivitymethod in finite element-model updating: A tutorial. Mech Syst Signal Process 2011;25(7):2275–96. http://dx.doi.org/10.1016/j.ymssp.2010.10.012.

[6] Salachoris GP, Standoli G, Betti M, Milani G, Clementi F. Evolutionary numerical model for cultural heritage structures via genetic algorithms: a case study in central Italy. Bull Earthq Eng 2023;1–35. http://dx.doi.org/10.1007/s10518-023-01615-z.

[7] Ereiz S, Duvnjak I, Fernando Jiménez-Alonso J. Review of finite element model updating methods for structural applications. Structures 2022;41:684–723. http://dx.doi.org/10.1016/j.istruc.2022.05.041.

[8] Monchetti S, Viscardi C, Betti M, Bartoli G. Bayesian-based model updating using natural frequency data for historic masonry towers. Probab Eng Mech 2022;70:103337. http://dx.doi.org/10.1016/j.probengmech.2022.103337.

[9] Monchetti S, Viscardi C, Betti M, Clementi F. Comparison between bayesian updating and approximate bayesian computation for model identification of masonry towers through dynamic data. Bull Earthq Eng 2023;1–19. http://dx.doi.org/10.1007/s10518-023-01670-6.

[10] Jiménez-Alonso JF, Naranjo-Pérez J, Pavic A, Sáez A. Maximum likelihood finite-element model updating of civil engineering structures using nature-inspired computational algorithms. Struct Eng Int 2020;31:1–13. http://dx.doi.org/10.1080/10168664.2020.1768812.

[11] Shabbir F, Omenzetter P. Model updating using genetic algorithms with sequential niche technique. Eng Struct 2016;120:166–82. http://dx.doi.org/10.1016/j.engstruct.2016.04.028.

[12] Costa C, Ribeiro D, Jorge P, Silva R, Arêde A, Calçada R. Calibration of the numerical model of a stone masonry railway bridge based on experimentally identified modal parameters. Eng Struct 2016;123:354–71. http://dx.doi.org/10.1016/j.engstruct.2016.05.044.

[13] Lacanna G, Betti M, Ripepe M, Bartoli G. Dynamic identification as a tool to constrain numericalmodels for structural analysis of historical buildings. Front Built Environ 2020;6. http://dx.doi.org/10.3389/fbuil.2020.00040.

[14] Girardi M, Padovani C, Pellegrini D, Robol L. A finite element model updating method based on global optimization. Mech Syst Signal Process 2021;107372. http://dx.doi.org/10.1016/j.ymssp.2020.107372.

[15] Liang JJ, Zhu XP, Yue CT, Li Z, Qu B. Performance analysis on knee point selection methods for multi-objective sparse optimization problems. In: 2018 IEEE congress on evolutionary computation. 2018, p. 1–8. http://dx.doi.org/10.1109/CEC.2018.8477915.

[16] Astroza R, Nguyen LT, Nestorovic T. Finite element model updating using simulated annealing hybridized with unscented Kalman filter. Comput Struct 2016;177:176–91. http://dx.doi.org/10.1016/j.compstruc.2016.09.001.

[17] Jin S-S, Jung H-J. Sequential surrogatemodeling for efficient finite element-model updating. Comput Struct 2016;168:30–45. http://dx.doi.org/10.1016/j.compstruc.2016.02.005.

[18] Lin K, Xu Y, Lu X, Guan Z, Li J. Cluster computing-aided model updating for a high-fidelity finite element model of a long-span cable-stayed bridge. Earthq Eng Struct Dyn 2020;49. http://dx.doi.org/10.1002/eqe.3270.

[19] Naranjo-Pérez J, Jiménez-Alonso JF, Pavic A, Sáez A. Finite-element-model updating of civil engineering structures using a hybrid UKF-HS algorithm. Struct Infrastruct Eng 2020;17(5):620–37. http://dx.doi.org/10.1080/15732479.2020.1760317.

[20] Naranjo-Pérez J, Infantes M, Jiménez-Alonso JF, Sáez A. A collaborative machine learning-optimization algorithm to improve the finite element model updating of civil engineering structures. Eng Struct 2020;225:111327. http://dx.doi.org/10.1016/j.engstruct.2020.111327.

[21] Allemang RJ, Brown DL. A correlation coefficient formodal vector analysis. 1982.

[22] Marwala T. Finite-element-model updating using computional intelligence techniques. Springer London; 2010, http://dx.doi.org/10.1007/978-1-84996-323-7.

[23] Naranjo-Pérez J, Jiménez-Alonso JF, Sáez A. Parameter identification of the dynamic winkler soil–structure interaction model using a hybrid unscented Kalman filter–multi-objective harmony search algorithm. Adv Struct Eng 2020;23(12):2653–68. http://dx.doi.org/10.1177/1369433220919074.

[24] Geem ZW, Kim JH, Loganathan G. A new heuristic optimization algorithm: Harmony search. Simulation 2001;76(2):60–8. http://dx.doi.org/10.1177/003754970107600201.
[25] Yang X-S, Koziel S, editors. Computational optimization and applications in engineering and industry. Springer Berlin Heidelberg; 2011, http://dx.doi.org/10.1007/978-3-642-20986-4.
[26] Deb K, Agrawal S, Pratap A, Meyarivan T. A fast and elitist multiobjective genetic algorithm: Nsga-ii. IEEE Trans Evol Comput 2002;6:182–97.
[27] Julier SJ, Uhlmann JK. New extension of the Kalman filter to nonlinear systems. In: Defense, security, and sensing. 1997.
[28] Wan E, Van Der Merwe R. The unscented Kalman filter for nonlinear estimation. In: Proceedings of the IEEE 2000 adaptive systems for signal processing, communications, and control symposium(Cat. no. 00EX373). 2000, p. 153–8. http://dx.doi.org/10.1109/ASSPCC.2000.882463.
[29] Tarantola A. Inverse problem theory and methods for model parameter estimation. Society for Industrial and Applied Mathematics; 2005, http://dx.doi.org/10.1137/1.9780898717921.
[30] Julier S, Uhlmann J. Corrections to unscented filtering and nonlinear estimation. Proc IEEE 2004;92(12):1958. http://dx.doi.org/10.1109/JPROC.2004.837637.
[31] Van der Merwe R, Wan E. The square-root unscented Kalman filter for state and parameter-estimation. In: 2001 IEEE international conference on acoustics, speech, and signal processing. proceedings (Cat. no. 01CH37221), vol. 6. 2001, p. 3461–4. http://dx.doi.org/10.1109/ICASSP.2001.940586.
[32] Terejanu G. Unscented Kalman filter tutorial. Univ Buffalo Buffalo; 2011.
[33] James G, Witten D, Hastie T, Tibshirani R. An introduction to statistical learning: With applications in R. 2013.
[34] Cybenko G. Approximation by superpositions of a sigmoidal function. Math Control Signals Systems 1989;2(4):303–14. http://dx.doi.org/10.1007/BF02551274.
[35] ichi Funahashi K. On the approximate realization of continuousmappings by neural networks. Neural Netw 1989;2:183–92.
[36] Hagan M, Menhaj M. Training feedforward networks with the marquardt algorithm. IEEE Trans Neural Netw 1994;5(6):989–93. http://dx.doi.org/10.1109/72.329697.
[37] Nocedal J, Wright SJ, editors. Numerical optimization. Springer-Verlag; 1999, http://dx.doi.org/10.1007/b98874.
[38] SPS. Sandwich plate systemheavy engineering composite fromintelligent engineering. 2023.
[39] Hudson E, Reynolds P. Design and construction of a reconfigurable pedestrian structure. Exp Tech 2016;41. http://dx.doi.org/10.1007/s40799-016-0144-3.
[40] AR140. ANSYS user's manual. 2011.
[41] Maia N, Silva J. Theoretical and experimental modal analysis. Engineering dynamics series, Research Studies Press; 1997.
[42] Fox RL, Kapoor MP. Rates of change of eigenvalues and eigenvectors. AIAA J 1968;6(12):2426–9. http://dx.doi.org/10.2514/3.5008.
[43] Jiménez-Alonso JF, Sáez A, Pavic A, Hudson J. Maximum likelihood methods for finite elementmodel updating of civil engineering structures: A comparative study. In: Proceedings of the 4th international conference on mechanical models in structural engineering cMMoST 2017. 2017, p. 519–32.
[44] Kermanshahi B. Design and application of neural networks. Shokodo Tokyo; 1999.
[45] Martínez A. Iglesia de san jerónimo (granada), URL http://www.ual.es/ideimand/iglesia-de-san-jeronimo-granada/.
[46] Augenti N, Parisi F, Acconcia E. Mada: online experimental database for mechanical modelling of existing masonry assemblages. 2012.
[47] Solutions SV. Artemis modal 5.0. user's guide. 2015.
[48] Wang T, Celik O, Catbas N, Zhang L. A frequency and spatial domain decomposition method for operational strain modal analysis and its application. Eng Struct 2016;27:62–6. http://dx.doi.org/10.1016/j.engstruct.2016.02.011.
[49] Peeters B, De Roeck G. Stochastic system identification for operational modal analysis: A review. Trans ASME, J Dyn Syst Meas Control 2001;123. http://dx.doi.org/10.1115/1.1410370.